Representing Graphs and Hypergraphs by Touching Polygons in 3D

William Evans[1] *Paweł Rzążewski*[2,3] *Noushin Saeedi*[1]
Chan-Su Shin[4] *Alexander Wolff*[5]

[1]University of British Columbia, Vancouver, Canada
[2]Warsaw University of Technology,
Faculty of Mathematics and Information Science, Warszawa, Poland
[3]Institute of Informatics, University of Warsaw, Warszawa, Poland
[4]Hankuk University of Foreign Studies, Yongin, Republic of Korea
[5]Universität Würzburg, Würzburg, Germany

Dedicated to Honza Kratochvíl on his 60th birthday.

Abstract

Contact representations of graphs have a long history. Most research has focused on problems in 2D, but 3D contact representations have also been investigated, mostly concerning fully-dimensional geometric objects such as spheres or cubes. In this paper we study contact representations with convex polygons in 3D. We show that every graph admits such a representation. Since our representations use super-polynomial coordinates, we also construct representations on grids of polynomial size for specific graph classes (bipartite, subcubic). For hypergraphs, we represent their duals, that is, each vertex is represented by a point and each edge by a polygon. We show that even regular and quite small hypergraphs do not admit such representations. On the other hand, the two smallest Steiner triple systems can be represented.

1   Introduction

Representing graphs as the contact of geometric objects has been an area of active research for many years (see Hliněný and Kratochvíl's survey [16] and Alam's thesis [1]). Most of this work concerns representations in 2D, though there has been some interest in three-dimensional representation as well [2, 3, 5, 14, 26]. Representations in 3D typically use 3D geometric objects that touch properly, i.e., their intersection is a positive area 2D face. In contrast, our main focus is on contact representation of graphs and hypergraphs using non-intersecting (open, "filled") planar polygons in 3D. Two polygons are in *contact* if they share a corner point. Note that two triangles that share two corner points do not intersect and a triangle and rectangle that share two corners, even diagonally opposite ones, also do not intersect. However, no polygon contains a corner of another except at its own corner. A *contact representation of a graph in 3D* is a set of non-intersecting polygons in 3D that represent vertices. Two polygons share a corner point if and only if they represent adjacent vertices and each corner point corresponds to a distinct edge. We can see a contact representation of a graph $G = (V, E)$ as a certain drawing of its *dual hypergraph* $H_G = (E, \{E(v) \mid v \in V\})$ which has a vertex for every edge of G, and a hyperedge for every vertex v of G, namely the set $E(v)$ of edges incident to v. We extend this idea to arbitrary hypergraphs: A *non-crossing drawing of a hypergraph in 3D* is a set of non-intersecting polygons in 3D that represent *edges*. Two polygons share a corner point if and only if they represent edges that contain the same vertex and each corner point corresponds to a distinct vertex. It is straightforward to observe that the set of contact representations of a graph G is the same as the set of non-crossing drawings of H_G.

Many people have studied ways to represent hypergraphs geometrically [4, 6, 18], perhaps starting with Zykov [31]. A natural motivation of this line of research was to find a nice way to represent combinatorial configurations [15] such as Steiner systems (for an example, see Fig. 15). The main focus in representing hypergraphs, however, was on drawings in the plane. By using polygons to represent hyperedges in 3D, we gain some additional flexibility though still not all hypergraphs can be realized. Our work is related to Carmesin's work [9] on a Kuratowski-type characterization of 2D simplicial complexes (sets composed of points, line segments, and triangles) that have an embedding in 3-space. Our representations are sets of planar polygons (not just triangles) that arise from hypergraphs. Thus they are less expressive than Carmesin's topological 2D simplicial complexes and are more restricted. In particular, if two hyperedges share three vertices, the hyperedges must be coplanar in our representation.

Our work is also related to that of Ossona de Mendez [22]. He showed that a hypergraph whose vertex–hyperedge inclusion order has poset dimension d can be embedded into $\mathbb{R}^{d-1}$ such that every vertex corresponds to a unique point in $\mathbb{R}^{d-1}$ and every hyperedge corresponds to the convex hull of its vertices. The embedding ensures that the image of a hyperedge does not contain the image of a vertex and, for any two hyperedges e and e', the convex hulls of $e \setminus e'$ and of $e' \setminus e$ don't intersect. In particular, the images of disjoint hyperedges are disjoint.

Table 1: Required grid volume and running times of our algorithms for drawing n-vertex graphs of certain graph classes in 3D

Graph class	general	bipartite	1-plane cubic	2-edge-conn. cubic	subcubic
Volume	super-poly	$O(n^4)$	$O(n^2)$	$O(n^2)$	$O(n^3)$
Runtime	$O(n^2)$	linear	linear	$O(n \log^2 n)$	$O(n \log^2 n)$
Reference	Thm. 2.3	Thm. 2.6	Thm. 2.8	Lem. 2.9	Thm. 2.10

Note that both Ossona de Mendez and we use triangles to represent hyperedges of size 3, but for larger hyperedges, he uses higher-dimensional convex subspaces. Note also that the method of Ossona de Mendez may insist on a higher dimension than actually needed. For example, every graph (seen as a 2-uniform hypergraph) can be drawn with non-intersecting straight-line segments in 3D, but the vertex–hyperedge inclusion order of K_{13} has poset dimension 5 [17], so the method of Ossona de Mendez needs 4D for a straight-line drawing of K_{13}.

Our contribution.   All of our representations in this paper use convex polygons while our proofs of non-representability hold even permitting non-convex polygons. We first show that recognizing segment graphs in 3D is $\exists\mathbb{R}$-complete.

We show that every graph on n vertices with minimum vertex-degree 3 has a contact representation by convex polygons in 3D, though the volume of the drawing using integer coordinates is at least exponential in n; see Section 2.

For some graph classes, we give 3D drawing algorithms which require polynomial volume. Table 1 summarizes our results. When we specify the volume of the drawing, we take the product of the number of grid lines in each dimension (rather than the volume of a bounding box), so that a drawing in the xy-plane has non-zero volume. Some graphs, such as the squares of even cycles, have particularly nice representations using only unit squares; see Fig. 14(a).

For hypergraphs our results are more preliminary. There are examples as simple as the hypergraph on six vertices with all triples of vertices as hyperedges that cannot be drawn using non-intersecting triangles; see Section 3. We show that hypergraphs with too many edges of cardinality 4 such as Steiner quadruple systems do not admit non-crossing drawings using convex quadrilaterals (they in fact do not admit non-crossing drawings with any quadrilaterals if the number of vertices is sufficiently large). On the other hand, we show that the two smallest Steiner triple systems can be drawn using triangles. (We define these two classes of hypergraphs in Section 3.)

2   Graphs

It is easy to draw graphs in 3D using points as vertices and non-crossing line segments as edges – any set of points in general position (no three collinear and

no four coplanar) will support any set of edge segments without crossings. A more difficult problem is to represent a graph in 3D using polygons as vertices where two polygons intersect to indicate an edge (note that here we do not insist on a *c*ontact representation, i.e., polygons are allowed to intersect arbitrarily). Intersection graphs of convex polygons in 2D have been studied extensively [27]. Recognition is $\exists\mathbb{R}$-complete [24] (and thus in PSPACE since $\exists\mathbb{R} \subseteq$ PSPACE [7]) even for segments (polygons with only two vertices).

Every complete graph trivially admits an intersection representation by line segments in 2D. Not every graph, however, can be represented in this way, see e.g., Kratochvíl and Matoušek [20]. Moreover, they show that recognizing intersection graphs of line segments in the plane, called *segment graphs*, is $\exists\mathbb{R}$-complete. It turns out that a similar hardness result holds for recognizing intersection graphs of straight-line segments in 3D (and actually in any dimension). The proof modifies the corresponding proof for 2D by Schaefer [24]. See also the excellent exposition of the proof by Matoušek [21].

Theorem 2.1 *Recognizing segment graphs in 3D is $\exists\mathbb{R}$-complete.*

Proof: Clearly the problem is in $\exists\mathbb{R}$, so we immediately turn to hardness. The proof is a reduction from STRETCHABILITY, where we are given a combinatorial description of a collection of pseudolines, and we ask whether there is a collection of straight lines with the same description.

We start with a brief description of the original reduction, in the 2-dimensional case [21, 24]. Following Schaefer and Matoušek, we will describe the construction geometrically. This is a convenient way to describe how to obtain a graph G from the combinatorial description of the collection of pseudolines so that G is a segment intersection graph if and only if the collection of pseudolines is stretchable. More specifically, we will assume that the input combinatorial description can be arranged by straight lines, and will describe a corresponding arrangement of straight-line segments, which forms an intersection representation of the constructed graph G. Formally, the input of the recognition problem is the purely combinatorial description of the graph G, not the representation. The construction ensures that if G is a segment intersection graph, then every intersection representation by segments must be equivalent to the intended one.

In his reduction, Schaeffer [21, 24] constructs an arrangement of segments with the desired combinatorial description. We call the segments in this arrangement *original segments*. He introduces three new, pairwise intersecting segments a, b, and c, called *frame segments*. They are placed in such a way that every original segment intersects at least two frame segments, and all intersections of original segments take place inside the triangle bounded by a, b, and c; see Fig. 1. Next, for every original segment, he adds many new segments, called *order segments*. Their purpose is to ensure that every representation of the constructed graph G with intersecting segments has the desired ordering of crossings of original segments; see Fig. 2 (left).

In order to show recognition hardness in 3D, we introduce some new segments (new vertices to G), obtaining a new graph G'. For each original segment s, we
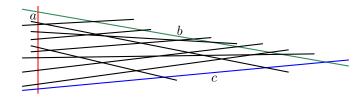
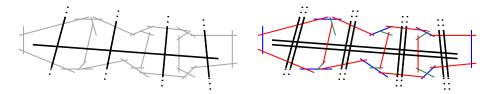Figure 1: Original segments and frame segments.

Figure 2: Left: Placement of order segments (thin lines). Original segments and frame segments are drawn with thick lines. Right: Twins force all segments to be coplanar. Each segment drawn red intersects two original or twin segments. Each segment drawn blue intersects two red segments. Finally, each green segment intersects a blue and a red segment.

introduce its *twin* s', i.e., a parallel non-overlapping segment with exactly the same neighbors as s. This completes the construction of G'.

Now we argue that in every representation of G', all segments from the representation are coplanar. First, note that the frame segments define a plane, let us call it the *base plane*. Moreover, recall that each original segment intersects at least two frame segments, so it also lies in the base plane. By the same argument, also twins of original segments lie in the base plane. Next, note that each order segment that intersects an original segment of G now intersects an original segment and its twin, which forces it to lie in the base plane. It is straightforward to verify that all other order segments are forced to lie in the base plane too; see Fig. 2 (right).

It is easy to verify (see, e.g., [8] for a similar argument) that G' can be represented by intersecting segments in 3D if and only if G' (and also G) can be represented by intersecting segments in 2D, and consequently, if and only if the initial instance of STRETCHABILITY is a yes-instance. □

We consider *contact representations* of graphs in 3D where no polygons are allowed to intersect except at their corners, and two polygons share a corner if and only if they represent adjacent vertices. We start by describing how to construct a contact representation for any graph using convex polygons, which requires at least exponential volume, and then describe constructions for graph families that use only polynomial volume.
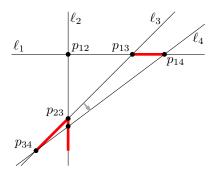
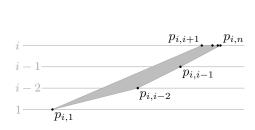Figure 3: Construction of ℓ_4 in the proof of Lemma 2.2.

Figure 4: The polygon P_i that represents vertex i of K_n.

2.1 General Graphs

Lemma 2.2 *For every positive integer $n \geq 3$, there exists an arrangement of n lines $\ell_1, \ell_2, \ldots, \ell_n$ with the following two properties:*

(A1) line ℓ_i intersects lines $\ell_1, \ell_2, \ldots, \ell_{i-1}, \ell_{i+1}, \ldots \ell_n$ in this order, and

(A2) distances between the intersection points on line ℓ_i decrease exponentially, i.e., for every i it holds that

$$d_i(j+2, j+1) \leq d_i(j+1, j)/2 \qquad for\ j \in \{1, \ldots, i-3\} \tag{1}$$
$$d_i(i+1, i-1) \leq d_i(i-1, i-2)/2 \tag{2}$$
$$d_i(i+2, i+1) \leq d_i(i+1, i-1)/2 \tag{3}$$
$$d_i(j+2, j+1) \leq d_i(j+1, j)/2 \qquad for\ j \in \{i+1, \ldots, n-2\}, \tag{4}$$

where $d_i(j, k)$ is the xy-plane distance between $p_{i,j}$ and $p_{i,k}$ and $p_{i,j} = p_{j,i}$ is the intersection point of ℓ_i and ℓ_j.

Proof: We construct the grid incrementally. We start with the x-axis as ℓ_1, the y-axis as ℓ_2, and the line through $(1, 0)$ and $(0, -1)$ as ℓ_3; see Fig. 3. Now suppose that $i > 3$, we have constructed lines $\ell_1, \ell_2, \ldots, \ell_{i-1}$, and we want to construct ℓ_i. We fix $p_{i-1,i}$ to satisfy $d_{i-1}(i, i-2) = d_{i-1}(i-2, i-3)/2$ then rotate a copy of line ℓ_{i-1} clockwise around $p_{i-1,i}$ until it (as ℓ_i) satisfies another of the inequalities in (1) with equality. Note that during this rotation, all inequalities in (A2) are satisfied and we do not move any previously constructed lines, so the claim of the lemma follows. $\square$

Theorem 2.3 *For every $n \geq 3$, the complete graph K_n admits a contact representation by non-degenerate convex polygons in 3D, each with at most $n - 1$ vertices. Such a representation can be computed in $O(n^2)$ time (assuming unit cost for arithmetic operations on coordinates).*

Proof: Take a grid according to Lemma 2.2 (thus, each line ℓ_i is in the xy-plane). We lift each intersection point $p_{i,j}$ so that the z-coordinate of $p_{i,j}$ becomes $\min\{i,j\}$. We represent vertex i by polygon P_i, which we define to be the convex hull of $\{p_{i,1}, p_{i,2}, \ldots, p_{i,i-1}, p_{i,i+1}, \ldots, p_{i,n}\}$. Note that P_i is contained in the vertical plane that contains line ℓ_i; see Fig. 4. To avoid that P_1 is degenerate, we reduce the z-coordinate of $p_{1,2}$ slightly.

We claim that the counterclockwise order of vertices around P_i, for $i = 2, \ldots, n-1$ is

$$p_{i,1}, p_{i,2}, \ldots, p_{i,i-1}, p_{i,n}, p_{i,n-1}, \ldots, p_{i,i+1}, p_{i,1}.$$

Similarly, we claim that the counterclockwise order of vertices around P_1 is $p_{1,2}, p_{1,n}, \ldots, p_{1,3}, p_{1,2}$, and the order around P_n is $p_{n,1}, p_{n,2}, \ldots, p_{n,n-1}, p_{n,1}$. Note that a polygon with such an ordering is simple (i.e., it does not self-intersect). We prove these claims by showing that the angle formed by any three consecutive points in these orders is bounded by π. We can easily verify this for P_1 and P_n. In the following we assume that $i \in \{2, \ldots, n-1\}$. Clearly the angles $\angle p_{i,i+1} p_{i,1} p_{i,2}$ and $\angle p_{i,i-1} p_{i,n} p_{i,n-1}$ are at most π. For $j = 2, \ldots, i-2$, we have $\angle p_{i,j-1} p_{i,j} p_{i,j+1} < \pi$, which is due to the fact that the z-coordinates increase in each step by 1, while the distances decrease (property (A2)). Note that $\angle p_{i,i+1}, p_{i,i+2}, p_{i,i+3} = \cdots = \angle p_{i,n-2}, p_{i,n-1}, p_{i,n} = \pi$. Finally, we claim that $\angle p_{i,i-2}, p_{i,i-1}, p_{i,n} < \pi$. Clearly, $z(p_{i,i-1}) - z(p_{i,i-2}) = 1 = z(p_{i,n}) - z(p_{i,i-1})$, where $z(p)$ denotes the z-coordinate of point p. The claim follows by observing that, due to property (A2) and the geometric series formed by the distances,

$$d_i(i-1,n) = d_i(i-1,i+1) + \sum_{k=i+1}^{n-1} d_i(k,k+1) < 2d_i(i-1,i+1) \le d_i(i-2,i-1).$$

It remains to show that, for $1 \le i < j \le n$, polygons P_i and P_j do not intersect other than in $p_{i,j}$. This is simply due to the fact that P_j is above P_i in $p_{i,j}$, and lines ℓ_i and ℓ_j only intersect in (the projection of) this point. $\qquad\square$

Corollary 2.4 *Every graph with minimum vertex-degree 3 admits a contact representation by convex polygons in 3D.*

Proof: Let n be the number of vertices of the given graph $G = (V, E)$. We use the contact representation of K_n and modify it as follows. For every pair $\{i, j\} \notin E$, just remove the point $p_{i,j}$ before defining the convex hulls.

In the above construction for K_n, we had to make sure that polygon P_1 is not degenerate. For general graphs, we have the same problem for any polygon P_i with the property that every polygon P_j that is adjacent to P_i has index $j > i$. Let k be the smallest index such that P_k is incident to P_i. Now if $k > i$ then we slightly reduce the z-coordinate of $p_{i,k}$. (In the construction for K_n, we did this only to $p_{1,2}$.) $\qquad\square$

We can make the convex polygons of our construction strictly convex if we slightly change the z-coordinates. For example, decrease the z-coordinate of $p_{i,j}$

by $\delta/d_{\min\{i,j\}}(1, \max\{i, j\})$, where $\delta > 0$ is such that moving every point by at most δ does not change the orientation of any three non-collinear points.

Let us point out that Erickson and Kim [12] describe a construction of pairwise face-touching 3-polytopes in 3D that may provide the basis for a different representation in our model of a complete graph.

While we have shown that all graphs admit a 3D contact representation, these representations may be very non-symmetric and can have very large coordinates. This motivates the following question and specialized 3D drawing algorithms for certain classes of (non-planar) graphs; see the following subsections.

Open Problem 2.5 *Is there a polynomial p such that any n-vertex graph has a 3D contact representation with convex polygons on a grid of size $p(n)$?*

2.2   Bipartite Graphs

Theorem 2.6 *Every bipartite graph $G = (A \cup B, E)$ admits a contact representation by convex polygons whose vertices are restricted to*

(a) a toroidal grid of size $|B| \times (2|A| - 2)$ or

(b) a 3D integer grid of size $|A| \times 2 \left\lceil \frac{|B|}{4} \right\rceil \times \left(\left\lceil \frac{|A|}{2} \right\rceil^2 + \left\lceil \frac{|B|}{4} \right\rceil^2 \right)$.

Such representations can be computed in $O(|E|)$ time.

Proof: We first prove the result for complete bipartite graphs $K_{|A|,|B|}$. As in the other costructions in this paper, our representation for $K_{|A|,|B|}$ is such that each polygon representing a vertex v of the graph is the convex hull of the touching points with adjacent polygons. (The touching points represent the edges of the graph.) If the given bipartite graph G is not complete, we simply remove from our representation of $K_{|A|,|B|}$ the touching points that correspond to the non-edges in G.

In our construction for $K_{|A|,|B|}$, the polygons representing the vertices in A (called *A-polygons*) are all horizontal $|B|$-gons and the polygons representing the vertices in B (called *B-polygons*) are all vertical $|A|$-gons; see Fig. 5 for an example with $|A| = |B| = 8$.

We start with a *uni-monotone* convex polygon with respect to the z-axis (that is, a z-monotone convex polygon with a single segment as one of its two chains) as our *lead* for generating a realization. For a uni-monotone polygon, we call the single edge monotone chain the *base edge* and the other chain the *mountain chain*. Our lead polygon represents a B-polygon (hence, is an $|A|$-gon) and has the following two properties: (i) it is coplanar with the z-axis, and (ii) its mountain chain lies between the base segment and the z-axis. The remaining B-polygons are all rotated copies of the lead polygon around the z-axis (each with a distinct rotation angle). The A-polygons are horizontal and each at a different height, and hence they are interior-disjoint. B-polygons are also trivially interior-disjoint. The A- and B-polygons are interior-disjoint due

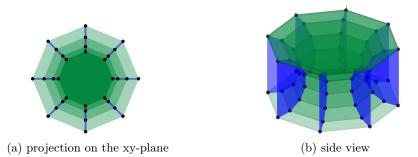(a) projection on the xy-plane   (b) side view

Figure 5: A contact representation of $K_{8,8}$ using a toroidal grid.

to property (ii) of our lead polygon. Using evenly spaced vertices on a half circle as our lead, we get a representation on a toroidal grid[1] of size $|B| \times (2|A| - 2)$ (note that our representation uses the inner half of the grid points of a toroidal grid because the lead polygon needs to be uni-monotone).

For representations on integer grids, we distort the representation above to some degree. A *core* A-polygon (innermost polygon in Fig. 6) is a convex $|B|$-gon on the xy-plane using a grid of size

$$2 \left\lceil \frac{|B|}{4} \right\rceil \times \left(\left\lfloor \frac{\left\lceil \frac{|B|}{2} \right\rceil}{2} \right\rfloor \left(\left\lceil \frac{|B|}{4} \right\rceil - 1 \right) + 2 \right).$$

Recall that the grid size is the product of the number of grid lines in each dimension. Here, we use both a core A-polygon, and a lead B-polygon (with additional properties), to generate a realization.

Our lead B-polygon has the following properties. It lies on the xz-plane and is to the right of the z-axis. It has an axis of symmetry parallel to the x-axis (this helps getting a more compact representation). The z-coordinates of consecutive vertices on its mountain chain are all one unit apart. The distance between the x-coordinates of consecutive pairs of vertices along the boundary and in the direction towards the base segment increments by $1, 2, 3, \ldots, \lceil |A|/2 \rceil - 1$. These properties guarantee that the lead polygon is uni-monotone, convex, and has integer coordinates. The lead B-polygon is incident to the leftmost vertex of the core A-polygon at its vertex with the minimum x-coordinate (i.e., closest to the z-axis).

The remaining B-polygons are again congruent, however, this time their planes are all parallel to the lead B-polygon (rather than being placed around the z-axis). This helps us maintain integer coordinates for all vertices. Figure 6 shows the projection of such representations on the xy-plane. Note that the core A-polygon can be split into two y-monotone chains of about the same size. The B-polygons that are incident to the vertices on the same y-monotone chain of the core are identical (only translated by a vector in the xy-plane). They

---

[1]A *toroidal grid* of size $m \times n$ is the Cartesian product of two cycle graphs C_m and C_n.
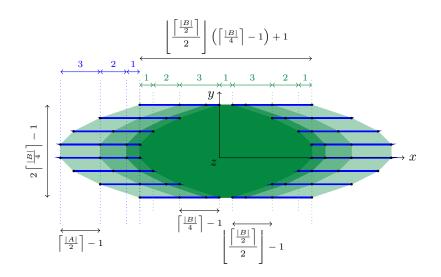
Figure 6: Top view of a contact representation of $K_{8,16}$ on the integer grid.
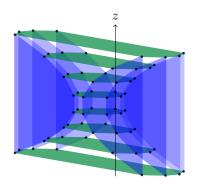

Figure 7: Side view of a contact representation of $K_{8,8}$ on the integer grid.

are mirrored if they are incident to vertices on different monotone chains of the core. See Fig. 7 for a 3D view of an example. Our construction requires a grid of size

$$|A| \times 2 \left\lceil \frac{|B|}{4} \right\rceil \times \left(\left\lceil \frac{|A|}{2} \right\rceil \left(\left\lceil \frac{|A|}{2} \right\rceil - 1 \right) + \left\lfloor \frac{\left\lceil \frac{|B|}{2} \right\rceil}{2} \right\rfloor \left(\left\lceil \frac{|B|}{4} \right\rceil - 1 \right) + 2 \right).$$

$\square$

Proposition 2.7 *The graph $K_{3,3}$ admits a contact representation in 3D using unit equilateral triangles.*

Proof: Our contact representation consists of three horizontal and three vertical unit equilateral triangles; see Fig. 8(a). The three horizontal triangles have z-

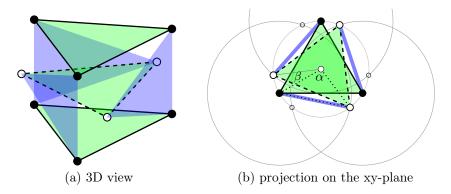(a) 3D view   (b) projection on the xy-plane

Figure 8: A contact representation of $K_{3,3}$ with unit equilateral triangles.
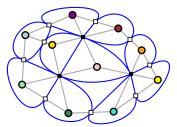
coordinates 0, 1/2, 1, and are centered at the z-axis. The topmost triangle is right above the bottommost one, whereas the middle triangle is rotated by an angle β. In the projection on the xy-plane, all their vertices lie on a circle of of radius $\tan(30°)$; see the small gray circle in Fig. 8(b). The figure also shows three big gray circles of radius $\sin(60°)$ (which is the height of a unit equilateral triangle) centered on the vertices of the top- and bottommost triangles. Each big circle intersects the small circle in two distinct points; in Fig. 8(b), the left one is marked with a small circle, the right one with a bigger circle. Connecting the right intersection points (bigger circles) yields the vertices of the middle horizontal triangle. The side lengths of the black dotted triangle are $\tan(30°)$, $\tan(30°)$, and $\sin(60°)$. By the law of cosines, $\alpha = 120° - \beta = \arccos(-1/8)$. Hence, $\beta \approx 22.82°$.   □
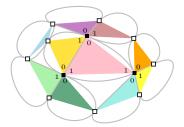
2.3   1-Planar Cubic Graphs

A simple consequence of the circle-packing theorem [19] is that every planar graph (of minimum degree 3) is the contact graph of convex polygons in the plane. In this section, we consider a generalization of planar graphs called *1-planar graphs* that have a drawing in 2D in which every edge (Jordan curve) is crossed at most once.

Our approach to realizing these graphs will use the *medial graph* G_{med} associated with a plane graph G (or, to be more general, with any graph that has an edge ordering). The vertices of G_{med} are the edges of G, and two vertices of G_{med} are adjacent if the corresponding edges of G are incident to the same vertex of G and consecutive in the circular ordering around that vertex. The medial graph is always 4-regular. If G has no degree-1 vertices, G_{med} has no loops. If G has minimum degree 3, G_{med} is simple. Also note that G_{med} is connected if and only if G is connected.

Theorem 2.8 *Every 1-plane cubic graph with n vertices can be realized as a contact graph of triangles with vertices on a grid of size $(3n/2-1)\times(3n/2-1)\times3$.*

(a) a 1-plane cubic graph G and its (modified) medial graph G'_{med}

(b) representation of G with triangles; the numbers indicate the z-coordinates of the triangle corners (unlabeled vertices lie in the xy-plane)

Figure 9: 1-plane cubic graphs admit compact triangle contact representations.

Given a 1-planar embedding of the graph, it takes linear time to construct such a realization.

Proof: Let G be the given 1-plane graph. Let G'_{med} be the medial graph of G with the slight modification that, for each pair $\{e, f\}$ of crossing edges, G'_{med} has only one vertex v_{ef}, which is incident to all (up to eight) edges that immediately precede or succeed e and f in the circular order around their endpoints; see Fig. 9(a). The order of the edges around v_{ef} is the obvious one. Using Schnyder's linear-time algorithm [25] for drawing 3-connected graphs[2] straight-line, we draw G'_{med} on a planar grid of size $(3n/2 - 1) \times (3n/2 - 1)$. Note that this is nearly a contact representation of G except that, in each crossing point, *all* triangles of the respective four vertices touch. Figure 9(b) is a sketch of the resulting drawing (without using Schnyder's algorithm) for the graph in Fig. 9(a).

  We add, for each crossing $\{e, f\}$, a copy v'_{ef} of the crossing point v_{ef} one unit above. Then we select an arbitrary one of the two edges, say $e = uv$. Finally we make the two triangles corresponding to u and v incident to v'_{ef} without modifying the coordinates of their other vertices. The labels in Fig. 9(b) are the resulting z-coordinates for our example; all unlabeled triangle vertices lie in the xy-plane.

  If a crossing is on the outer face of G, it can happen that a vertex of G incident to the crossing becomes the outer face of G'_{med}; see Fig. 10 where this vertex is called a and the crossing edges are ac and bd. Consider the triangle Δ_a that represents a in G'_{med}. It covers the whole drawing of G'_{med}. To avoid intersections with triangles that participate in other crossings, we put the vertex of Δ_a that represents the crossing to $z = -1$, together with the vertex of the triangle Δ_c that represents c.

  Our 3D drawing projects vertically back to the planar drawing, so all triangles are interior disjoint (with the possible exception of a triangle that represents

---

[2]If G'_{med} is not 3-connected, we add dummy edges to fully triangulate it and then remove these edges to obtain a drawing of G'_{med}.
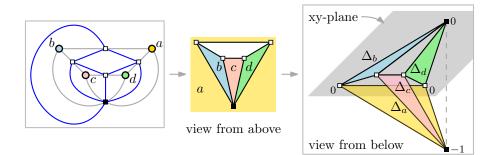
Figure 10: left: graphs G (with a crossing on the outer face) and G'_{med}; center: straight-line drawing of G'_{med}; right: resulting 3D representation of G (numbers are z-coordinates).

the outer face of G'_{med}). Triangles that share an edge in the projection are incident to the same crossing – but this means that at least one of the endpoints of the shared edge has a different z-coordinate. Hence, all triangle contacts are vertex–vertex contacts. Note that some triangles may touch each other at $z = 1/2$ (as the two central triangles in Fig. 9(b)), but our contact model tolerates this.   □

2.4   Cubic Graphs

We first solve a restricted case and then show how this helps us to solve the general case of cubic graphs.

Lemma 2.9 *Every 2-edge-connected cubic graph with n vertices can be realized as a contact graph of triangles with vertices on a grid of size $3 \times n/2 \times n/2$. It takes $O(n \log^2 n)$ time to construct such a realization.*

Proof: By Petersen's theorem [23], any given 2-edge-connected cubic graph G has a perfect matching. Note that removing this matching leaves a 2-regular graph, i.e., a set of vertex-disjoint cycles $C_1, \ldots, C_k$; see Fig. 11(a). Such a partition can be computed in $O(n \log^2 n)$ time [11]. Let $n = |V(G)|$ and $n_1 = |V(C_1)|, \ldots, n_k = |V(C_k)|$. Note that $n = n_1 + \cdots + n_k$. We now construct a planar graph $H = (V, E)$ with $n+1$ vertices that will be the "floorplan" for our drawing of G. The graph H consists of an n-wheel with outer cycle $v_{1,1}, \ldots, v_{1,n_1}, \ldots, v_{k,1}, \ldots, v_{k,n_k}$, n spokes and a hub h, with additional *chords* $v_{1,1}v_{1,n_1}, v_{2,1}v_{2,n_2}, \ldots, v_{k,1}v_{k,n_k}$. We call the edges $v_{1,n_1}v_{2,1}, \ldots, v_{k,n_k}v_{1,1}$ *dummy edges* (thin gray in Fig. 11(b) and (c)) and the other edges on the outer face of the wheel *cycle edges*.

The chords and cycle edges form triangles with apex h. More precisely, for every $i \in \{1, \ldots, k\}$, the chord-based triangle $\Delta v_{i,1}v_{i,n_i}h$ and the $n_i - 1$ cycle-based triangles $\Delta v_{i,1}v_{i,2}h, \ldots, \Delta v_{i,n_i-1}v_{i,n_i}h$ together represent the n_i vertices in the cycle C_i of G. For each C_i, we still have the freedom to choose which
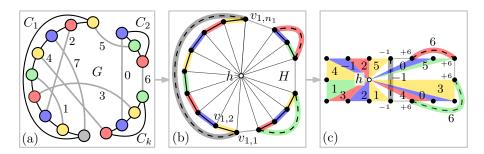
Figure 11: Representing a 2-edge-connected cubic graph G by touching triangles in 3D: (a) partition of the edge set into disjoint cycles and a perfect matching (the numbers denote a permutation of the matching edges); (b) the graph H; (c) 3D contact representation of G; the numbers inside the triangles indicate the z-coordinates of the triangle apexes (above h), the small numbers denote the non-zero z-coordinates of the vertices.

vertex of G will be mapped to the chord-based triangle of H. This will depend on the perfect matching in G. The cycle edges will be drawn in the xy-plane (except for those incident to a chord edge); their apexes will be placed at various grid points above h such that matching triangles touch each other. The chord-based triangles will be drawn horizontally, but not in the xy-plane.

In order to determine the height of the triangle apexes, we go through the edges of the perfect matching in an arbitrary order; see the numbers in Fig. 11(a). Whenever an endpoint v of the current edge e is the *last* vertex of a cycle, we represent v by a triangle with chord base. We place the apexes of the two triangles that represent e at the lowest free grid point above h; see the numbers in Fig. 11(c). Our placement ensures that, in every cycle (except possibly one, to be determined later), the chord-based triangle is the topmost horizontal triangle; all cycle-based triangles are below it. This guarantees that the interiors of no two triangles intersect (and the triangles of adjacent vertices touch).

Now we remove the chords from H. The resulting graph is a wheel; we can simply draw the outer cycle using grid points on the boundary of a $(3 \times n/2)$-rectangle and the hub on any grid point in the interior. (For the smallest cubic graph, K_4, we would actually need a (3×3)-rectangle, counting grid lines, in order to have a grid point in the interior, but it's not hard to see that K_4 can be realized on a grid of size $3 \times 2 \times 2$.) If one of the k cycles encloses h in the drawing (as C_1 in Fig. 11(c)), we move its chord-based triangle from $z = z^\star > 0$ to the plane $z = -1$, that is, below all other triangles. Let $i^\star$ be the index of this cycle (if it exists). Note that this also moves the apex of the triangle that is matched to the chord-based triangle from $z = z^\star$ to $z = -1$. In order to keep the drawing compact, we move each apex with z-coordinate $z' > z^\star$ to $z' - 1$. Then the height of our drawing equals exactly the number of edges in the perfect matching, that is, $n/2$.

The correctness of our representation follows from the fact that, in the orthogonal projection onto the xy-plane, the only pairs of triangles that overlap are the pairs formed by a chord-based triangle with each of the triangles in its cycle and, if it exists, the chord-based triangle of $C_{i^\star}$ with all triangles of the other cycles. Also note that two triangles $\Delta v_{i,j-1}v_{i,j}h$ and $\Delta v_{i,j}v_{i,j+1}h$ (the second indices are modulo n_i) that represent consecutive vertices in C_i (for some $i \in \{1,\ldots,k\}$ and $j \in \{1,\ldots,n_i\}$) touch only in a single point, namely in the image of $v_{i,j}$. This is due to the fact that vertices of G that are adjacent on C_i are not adjacent in the matching, and for each matched pair its two triangle apexes receive the same, unique z-coordinate.

We do not use all edges of H for our 3D contact representation of G. The spokes of the wheel are the projections of the triangle edges incident to h. The k dummy edges don't appear in the representation (but play a role in the proof of Theorem 2.10 ahead).   □

In order to generalize Lemma 2.9 to any cubic graph G, we use the *bridge-block tree* of G. This tree has a vertex for each 2-edge-connected component and an edge for each bridge of G. The bridge-block tree of a graph can be computed in time linear in the size of the graph [30]. The general idea of the construction is the following. First, remove all bridges from G and, using some local replacements, transform each connected component of the obtained graph into a 2-edge-connected cubic graph. Then, use Lemma 2.9 to construct a representation of each of these graphs. Finally, modify the obtained representations to undo the local replacements and use the bridge-block tree structure to connect the constructed subgraphs, restoring the bridges of G.

Theorem 2.10 *Every cubic graph with n vertices can be realized as a contact graph of triangles with vertices on a grid of size $3n/2 \times 3n/2 \times n/2$. It takes $O(n\log^2 n)$ time to construct such a realization.*

Proof: We can assume that the given graph G is connected, otherwise we draw each connected component separately and place the drawings side-by-side. Then the bridge-block tree of G yields a partition of G into 2-edge-connected components $G_1,\ldots,G_k$, which are connected to each other by bridges.

We go through $G_1,\ldots,G_k$ and construct floorplan graphs $H_1,\ldots,H_k$ as follows. If G_i is a single vertex, let H_i be a triangle. For an example, see H_6 in Fig. 12. If a component G_i with $n_i > 1$ doesn't contain any matching edge, that is, if all its vertices are endpoints of bridges, then let H_i be (an internally triangulated) n_i-cycle. The vertices in G_i will be represented by triangles whose bases are the edges of the cycle and whose apexes lie outside the cycle. Each apex v_b corresponds to a bridge b and will later be connected to a triangle representing the other endpoint of the bridge.

Otherwise, we remove each vertex in G_i that is incident to a bridge and connect its two neighbors, so that we can apply Petersen's theorem [23] to G_i. We call the new edge the *foot* of the bridge. This yields a collection of cycles and a perfect matching in G_i. As in the proof of Lemma 2.9, H_i is a wheel with $|V(G_i)|+1$ vertices, and we compute, for each component G_i, the heights of all
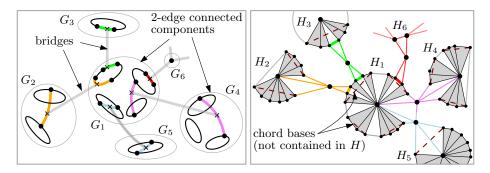
Figure 12: Constructing the floorplan H of a general cubic graph

triangle apexes. This also determines which vertices of G_i are represented by chord-based triangles. If applying Petersen's theorem to G_i gives rise to a single cycle, we consider the chord (which will be drawn at $z = -1$) to simultaneously be a dummy edge (which will be "drawn" at $z = 0$), so that every graph H_i has a dummy edge. (For examples, see H_3 or H_5 in Fig. 12.)

Let H be the disjoint union of $H_1, \ldots, H_k$. Now we reintroduce the bridges. For every bridge b, we add a new vertex v_b to H. Each foot of b is either a cycle edge or a matching edge in some G_i, which we treat differently; see Fig. 12.

If the foot uw of b is a cycle edge, consider the two adjacent triangles in H_i that share the vertex representing the foot uw. These triangles share the hub h_i of H_i and a vertex v_{uw} on the outer face of H_i. We take the two triangles apart by duplicating v_{uw}. We connect each copy of v_{uw} to the other copy, to v_b, to h_i, and to a different neighbor along the cycle. The new edges between the two copies and between them and v_b form a triangle that represents one of the two endpoints of the bridge b; see Fig. 13 (right).

If the foot uw of b is a matching edge, we pick a dummy edge xy on the outer face of H_i. Recall that dummy edges are the edges that connect the cycles in H_i (thin gray in Figs. 11(b) and (c)). Due to our construction, H_i contains at least one dummy edge. We remove the dummy edge xy and connect x, h_i, and y to v_b in this order. Note that several bridge feet can be placed into the space reserved by a single dummy edge (see the bridges that connect H_4 and H_5 to H_1 in Fig. 12 (right)).

Then we draw H in the xy-plane, using Schnyder's linear-time algorithm [25]. (In order to make H 3-connected, we add edges in the outer face of H that connect the components that are leaves of the bridge-block tree.) Finally, as in the proof of Lemma 2.9, we insert the chord edges (at the correct heights) and extend all cycle and chord edges into triangles by placing their apexes at the locations above or below h_i that we've computed before. Whenever we place two apexes that correspond to a matching edge that is the foot of a bridge b, we use two consecutive grid points, one for each apex. (If one of the apexes belongs to the chord-based triangle at $z = -1$, we place the other apex at $z = 0$.) Together with v_b (which remains on the xy-plane), the two apexes form a vertical triangle;
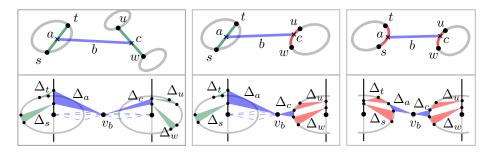
Figure 13: Representation of a bridge $b = ac$ depending on the types of its feet

see Fig. 13 (left). The projection of the triangle to the xy-plane is an edge of H; the vertical (closed) slab above that edge is used exclusively by the new triangle.

To bound the grid size of the drawing, we show that $|V(H)| \leq |E(G)|$ $(= 3n/2)$, by establishing an injective map from $V(H)$ to $E(G)$: we map every cycle vertex in H to the ccw next cycle edge in H, which corresponds to a specific cycle edge in G. Further, we map every bridge vertex v_b to the corresponding bridge b in G. It remains to map the hubs. If a component H_i of H does not contain any matching edge (that is, all vertices in H_i are incident to bridges), H_i does not contain a hub. Otherwise, there is at least one matching edge in H_i and we map the hub h_i to that edge.

Now it is clear that the straight-line drawing of H computed by Schnyder's algorithm has size at most $(3n/2 - 1) \times (3n/2 - 1)$. In order to bound the height of the drawing, consider any component H_i of H. Clearly, H_i contains at most $n/2$ matching edges. Each of these uses a grid point on the vertical line through h_i. Any matching edge can, however, be the foot of a bridge. For each bridge triangle that we insert between the apexes of two matching triangles, the height of the representation of H_i increases by one unit. On the other hand, the bridges form a matching that is independent from the matching edges. Thus, the height of H_i is at most $n/2$.   □

Corollary 2.11 *Every graph with n vertices and maximum degree 3 can be realized as a contact graph of triangles, line segments, and points whose vertices lie on a grid of size $3\lceil n/2 \rceil \times 3\lceil n/2 \rceil \times \lceil n/2 \rceil$. It takes $O(n \log^2 n)$ time to construct such a realization.*

Proof: If n is odd, add a dummy vertex to the given graph. Then add dummy edges until the graph is cubic. Apply Theorem 2.10. From the resulting representation, remove the triangle that corresponds to the dummy vertex, if any. Disconnect the pairs of triangles that correspond to dummy edges.   □

2.5   Squares of Cycles

Recall that, for an undirected graph G and an integer $k \geq 2$, the k-th *power* G^k of G is the graph with the same vertex set where two vertices are adjacent
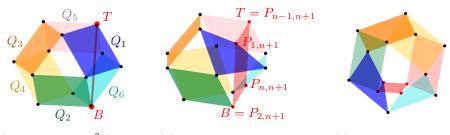
when their distance in G is at most k. Note that $C_4^2 = K_4$ is 3-regular (and can be represented by four unit equilateral triangles that pairwise touch and form an octahedron with four empty faces). For $n \geq 5$, C_n^2 is 4-regular. Recall that Corollary 2.4 yields contact representations using convex polygons for any graph, but in these representations the ratio between the length of the longest edge and the length of the shortest edge can be huge. For squares of cycles, we can do better.

Theorem 2.12 *For $n \geq 5$, C_n^2 admits a contact representation using convex quadrilaterals in 3D such that the ratio between the length of the longest edge and the length of the shortest edge over all quadrilateral edges in the representation is constant. For even n, the quadrilaterals can be unit squares.*

Proof: For even $n \geq 6$, C_n^2 is planar, so it is easy to find a contact representation with convex quadrilaterals in the plane. In 3D, however, we can restrict the quadrilaterals to unit squares; see Fig. 14(a). Note that the vertices on the middle plane form a regular n-gon and the vertices on the top and bottom planes form regular $(n/2)$-gons, all centered at the z-axis. Additionally, each vertex of the top or bottom plane lies on the bisector of the (empty) triangular face incident to it.

Finding a representation of $C_5^2 = K_5$ we leave as an exercise to the reader. Now we obtain a representation of C_{n+1}^2 from that of C_n^2 for even $n \geq 6$ (see Fig. 14 for an illustration of our construction for $n = 6$). Every vertex v_i in C_{n+1}^2 is represented by a quadrilateral Q_i. For two touching quadrilaterals Q_i and Q_j, let $P_{i,j}$ be their contact point (which represents the edge $v_i v_j$ in the graph C_{n+1}^2). Note that all edges of C_n^2 except for two, namely $v_1 v_{n-1}$ and $v_2 v_n$, are also edges in C_{n+1}^2. Moreover, the endpoints of these two non-edges of C_{n+1}^2 are all incident to v_{n+1}. Therefore, we can easily extend a contact representation of C_n^2 into one of C_{n+1}^2 as follows. Starting with a contact representation of C_n^2, we duplicate the vertices $T = P_{1,n-1}$ and $B = P_{2,n}$ (red in Fig. 14(a)) to separate the pairs (Q_1, Q_{n-1}) and (Q_2, Q_n) of touching quadrilaterals such that the four new vertices form the new quadrilateral Q_{n+1}.

In the following, we detail how we place the new vertices. We place $P_{n-1,n+1}$ and $P_{2,n+1}$ at the position of T and B respectively (thus Q_{n-1} and Q_2 do not change). Consider the four points T, B, and the centers of Q_1 and Q_n. Due to the symmetry of our representation for C_n^2, these four points span a plane H. Starting in T, we move $P_{1,n+1}$ along the line $H \cap Q_1$. We stop just before we reach the center of Q_1. Symmetrically, we define the position of $P_{n,n+1}$ along the line $H \cap Q_n$ near the center of Q_n. Stopping the movement before reaching the centers of Q_1 and Q_n makes sure that these faces remain strictly convex. In the resulting representation of C_{n+1}^2, every quadrilateral edge has length at most $|\overline{TB}| < 2$ and at least (nearly) $\sqrt{2}/2$, which implies that the ratio of the longest edge length and the shortest edge length is constant. □

(a) realization of C_6^2 (excluding the red segment)

(b) side view of a 3D realization of C_7^2

(c) top view of a 3D realization of C_7^2

Figure 14: Representing squares of cycles: we build a contact representation of C_7^2 from that of C_6^2. To this end, we split the two big (red) vertices to expand the segment connecting them into a rectangle.

3 Hypergraphs

We start with a negative result. Hypergraphs that give rise to simplicial 2-complexes that are not embeddable in 3-space also do not have a realization using touching polygons. Carmesin's example of the cone over the complete graph K_5 is such a 2-complex[3], which arises from the 3-uniform hypergraph on six vertices whose edges are $\{\{i,j,6\}\colon \{i,j\}\in [5]^2\}$. Recall that d-uniform means that all hyperedges have cardinality d. Any 3-uniform hypergraph that contains these edges also cannot be drawn. For example, $\mathcal{K}_n^d$, the complete d-uniform hypergraph on $n \geq 6$ vertices for $d = 3$ does not have a non-crossing drawing in 3D. Note that in complete hypergraphs many pairs of hyperedges share two vertices. This motivates us to consider 3-uniform *linear* hypergraphs, i.e., hypergraphs where pairs of edges intersect in at most one vertex. Very symmetric examples of such hypergraphs are *Steiner systems* (definition below).

3.1 Representing Steiner Systems by Touching Polygons

A Steiner system $S(t,k,n)$ is an n-element set S together with a set of k-element subsets of S (called *blocks*) such that each t-element subset of S is contained in exactly one block. In particular, Steiner triple systems $S(2,3,n)$ are examples of 3-uniform hypergraphs on n vertices; see Table 2 [29]. They exist for any $n \in \{6k + 1, 6k + 3\colon k \in \mathbb{N}\}$. The corresponding 3-uniform hypergraph has $n(n-1)/6$ hyperedges and is $((n-1)/2)$-regular.

First we show that the two smallest triple systems, i.e., $S(2,3,7)$ (also called the *Fano plane*) and $S(2,3,9)$, admit non-crossing drawings in 3D. The existence of such representations also follows from Ossona de Mendez' work [22] (see introduction) since both hypergraphs have incidence orders of dimension 4

---

[3]Carmesin [9] credits John Pardon with the observation that the *link graph* at a vertex v, which contains a node for every edge at v and an arc connecting two such nodes if they share a face at v, must be planar for the 2-complex to be embeddable.

Table 2: The two smallest Steiner triple and quadruple systems

$S(2,3,7)$	$S(2,3,9)$		$S(3,4,8)$		$S(3,4,10)$		
1 2 3	1 2 3	1 5 9	1 2 4 8	3 5 6 7	1 2 4 5	1 2 3 7	1 3 5 8
1 4 7	4 5 6	2 6 7	2 3 5 8	1 4 6 7	2 3 5 6	2 3 4 8	2 4 6 9
1 5 6	7 8 9	3 4 8	3 4 6 8	1 2 5 7	3 4 6 7	3 4 5 9	3 5 7 0
2 4 6	1 4 7	1 6 8	4 5 7 8	1 2 3 6	4 5 7 8	4 5 6 0	1 4 6 8
2 5 7	2 5 8	2 4 9	1 5 6 8	2 3 4 7	5 6 8 9	1 5 6 7	2 5 7 9
3 4 5	3 6 9	3 5 7	2 6 7 8	1 3 4 5	6 7 9 0	2 6 7 8	3 6 8 0
3 6 7			1 3 7 8	2 4 5 6	1 7 8 0	3 7 8 9	1 4 7 9
					1 2 8 9	4 8 9 0	2 5 8 0
					2 3 9 0	1 5 9 0	1 3 6 9
					1 3 4 0	1 2 6 0	2 4 7 0

(which can be checked by using an integer linear program). While our drawings have good vertex resolution (ratio between the smallest and the longest vertex–vertex distance) and show symmetries, Ossona de Mendez uses coordinates $1, d+1, (d+1)^2, \ldots, (d+1)^{n-1}$ in each of $d = 4$ dimensions and then projects this 4D contact representation centrally onto a 3D hyperspace. The resulting 3D contact representation does not lie on a grid.

Proposition 3.1 *The Fano plane $S(2,3,7)$ and the Steiner triple system $S(2,3,9)$ admit non-crossing drawings using triangles in 3D.*

Proof: We first describe our construction for the Fano plane, which has seven vertices and seven hyperedges; see Table 2 and Fig. 15. We start with a unit equilateral triangle on the xy-plane centered at the z-axis representing hyperedge 642 (with vertices in ccw-order). We make a copy of this triangle, lift it by one unit, and rotate it by an angle of α counterclockwise around the z-axis, where $0° < \alpha < 120°$ and $\alpha \neq 60°$ (Fig. 15 uses $\alpha = 85°$). The copied triangle is not a hyperedge but determines the position of vertices 3, 5, and 7 (i.e., after the transformation, vertices 6, 4, and 2 are mapped to vertices 3, 5, and 7, respectively). We place vertex 1 at $(0, 0, 1/2)$.

The three (green) triangles sharing vertex 1 are interior-disjoint for any α and are non-degenerate for $\alpha \neq 60°$. For $0° < \alpha < 120°$, the four (blue) triangles that are not incident to 1 are interior-disjoint and intersect no other triangles.

Now we turn to $S(2,3,9)$; see Table 2 and Fig. 17. We start with a unit equilateral triangle on the xy-plane centered at the z-axis representing hyperedge 852 (with vertices in ccw-order). We make a copy of this triangle, lift it up by one unit, rotate it by an angle β counterclockwise around the z-axis, and scale it from its center by the factor $1/5$. This gives us triangle 369. We place vertices 1 and 4 at $(0, 0, 3/4)$ and $(0, 0, 1/4)$, respectively. Figure 16 illustrates the triangles induced by these eight vertices.

It is easy to see that for any $\beta \leq 60°$, the (blue) triangles incident to vertex 4 are interior-disjoint. Suppose $\beta = 60°$. Then, in the projection on the xy-plane (through the z-axis), the (green) triangles incident to vertex 1 map to
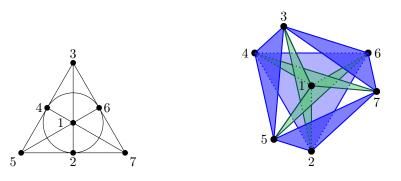
Figure 15: The Fano plane and a drawing using touching triangles in 3D

three segments all intersecting at the same point. Thus, in order for the green triangles to be interior-disjoint, we need $\beta < 60°$; and in fact the smaller the scale factor is (from one), the smaller β needs to be. Note that β cannot be too small, as otherwise the blue and green triangles would intersect. More precisely, β should be large enough so that for any two triangles $4uv$ and $1uw$, where $u \in \{2,5,8\}$ and $v, w \in \{3,6,9\}$, in the projection through the directed line $u4$, the projection of v is to the right of the projection of w and the projection of w is to the right of the projection of 1. In our construction, we use $\beta = 45°$ (and the scale factor $1/5$), which satisfies all the required conditions for having the blue and green triangles interior-disjoint. So far, we have determined the position of eight vertices (i.e., all but 7) such that the (eight) triangles induced by them are all pairwise non-intersecting.

Vertex 7 (not placed yet) forms four triangles with segments 26, 35, 89, and 14. Note that the first three of these segments are on the convex hull of the vertices put so far (see Fig. 16(b)). Let ℓ denote the intersection line of the planes defined by 358 and 269. The projection of ℓ and the projection of segment 89 on the xy-plane intersect (see Fig. 16(a)). Let H be the plane containing 89 and parallel to the z-axis, and let P be the intersection point of H and ℓ. If vertex 7 is above P, then the set of eight triangles not incident to 7, together with triangles 267, 357, and 789 are all pairwise non-intersecting (recall that segments 26, 35, and 67 are on the convex hull of vertices $\{1,\ldots,6,8,9\}$). In order to make sure that triangle 147 does not cause any intersections, we fix the position of 7 by lifting P slightly so that it still remains below the plane defined by 123. In our construction, 7 is obtained by lifting P by $1/10$ unit. Our drawing fits in a rectangular cuboid of size $1 \times 1 \times 1.5$. The minimum distance between any two vertices is $1/5$ in this drawing. Figure 17 illustrates a (complete) representation of $S(2,3,9)$. □

Now we turn to a special class of 4-uniform hypergraphs; Steiner quadruple systems $S(3,4,n)$ [28]. They exist for any vertex number in $\{6k+2, 6k+4 \colon k \in \mathbb{N}\}$. For $n = 8, 10, 14, \ldots$, the corresponding 4-uniform hypergraph has $m = \binom{n}{3}/4$ hyperedges and vertex degree $4m/n = (n-1)(n-2)/6$. In the following,
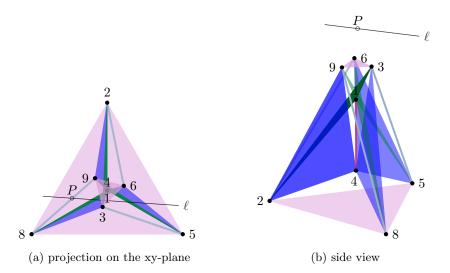
(a) projection on the xy-plane   (b) side view

Figure 16: Partial drawing of the Steiner triple system $S(2, 3, 9)$ showing triangles not incident to 7, together with the opposite segments to 7 for the remaining triangles.

we study the realizability of Steiner quadruple systems.

Observation 3.2 *In a non-crossing drawing of a Steiner quadruple system using quadrilaterals in 3D, every plane contains at most four vertices.*

Proof: Suppose that there is a drawing R and a plane Π that contains at least five vertices. Let ab be a maximum length edge of the convex hull of the points in the plane Π. No four, say $wxyz$ in that order, can be collinear, otherwise the quadrilateral containing wyz is either $wxyz$, which is degenerate (a line segment), or it contains x on its perimeter but x is not a corner, a contradiction. Thus the set S of vertices on Π that are not on the edge ab has size at least two. If there exist $u, v \in S$ such that abu and abv form[4] two distinct quadrilaterals with ab then these quadrilaterals intersect in the plane (they are both on the same side of ab), a contradiction. If no such pair exists then S contains exactly two points and they form one quadrilateral with ab, which must contain the other vertex in Π (on the edge ab) that is not a corner, a contradiction.   □

Observation 3.2 is the starting point for the following result.

Proposition 3.3 *The Steiner quadruple system $S(3, 4, 8)$ does not admit a non-crossing drawing using (convex or non-convex) quadrilaterals in 3D.*

Proof: The Steiner quadruple system $S(3, 4, 8)$ has eight vertices and 14 hyperedges and is unique; see Table 2.

---

[4]In a Steiner quadruple system, every triple of vertices appears in a unique quadruple.

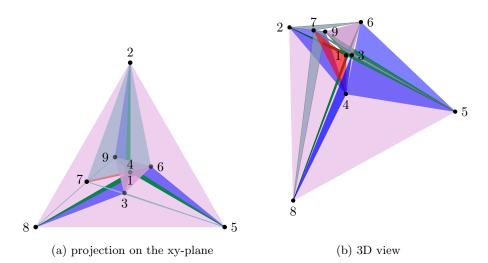(a) projection on the xy-plane   (b) 3D view

Figure 17: 3D contact representation of the Steiner triple system $S(2,3,9)$.

Assume that $S(3,4,8)$ has a contact representation by quadrilaterals. Without loss of generality, assume that quadrilateral 1248 lies on the xy-plane. We show that the supporting plane of the triple 367 is also the xy-plane, which, by Observation 3.2, is a contradiction.

The line through 18 and the line through 24 either intersect in a point v on the xy-plane or are parallel. The supporting planes of 1378 and 2347 both contain the line through 37 and the point v or, if v doesn't exist, the line 37 is parallel to 18 and 24. Similarly, the lines 14 and 28 intersect in a point w on the xy-plane or are parallel. The supporting planes of 1467 and 2678 both contain the line through 67 and the point w or, if w doesn't exist, the line 67 is parallel to 14 and 28. Again, a similar statement holds for the intersection u on the xy-plane of the lines 12 and 48. The supporting planes of 1236 and 3468 both contain the line 36 and the point u or, if u doesn't exist, the line 36 is parallel to 12 and 48. These conditions imply that the supporting plane of 367 is parallel to the xy-plane (unless 3, 6, and 7 are all collocated which is not possible as otherwise quadrilateral 3567 is a segment). Since at least one of u, v, and w exists and is in the xy-plane, 367 lies in the xy-plane, contradicting Observation 3.2.   □

The main observation used in proving Proposition 3.3 is that if we partition any quadruple $abcd$ into two pairs in any way, there exists a fixed pair, say ef, such that the union of ef and each of the two partitions form a quadruple in $S(3,4,8)$. We note that the same property holds for $S(3,4,10)$. However, since this case contains more vertices, the "fixed pairs" obtained from different ways of "partitioning" of a quadruple would not have common vertices, and hence this property alone is not enough to show that $S(3,4,10)$ cannot be realized. We show this for a restricted case using the following auxiliary lemma.

Lemma 3.4 *Let H be a hypergraph whose edge set contains the subset $F = \{abcd, abuv, cduv, acwx, bdwx, adyz, bcyz\}$. Then H does not admit a contact representation by quadrilaterals in which the edges in F are all convex or all non-convex.*

Proof: Suppose that H has a representation where the hyperedges in F are all convex. Let $e = abcd$. (Note that we identify e with the quadrilateral that represents it.) No matter which segments form the diagonals of e (ab and cd, ac and bd, or ad and bc), there is a pair (uv, wx, or yz) that forms two hyperedges with the two diagonals. We assume that the diagonals are ab and cd forming hyperedges $abuv$ and $cduv$. Due to the convexity of the quadrilateral e, ab and cd intersect. Hence, since $abuv$ and $cduv$ are convex, one of the hyperedges $abuv$ and $cduv$ must be drawn above e, and the other below e. This yields the desired contradiction since u and v are contained in both of these hyperedges.

Suppose that H has a representation where the hyperedges in F are all non-convex. We may assume that the diagonals of e are again ab and cd, that ab is not contained in e, and that c lies on the convex hull of e whereas d does not. Let x be the intersection point of the supporting lines of ab and cd. Note that x lies on ab. This is due to the fact that cd is incident to c and lies inside the angle $\angle acb$. The supporting planes of the quadrilaterals $abuv$ and $cduv$ intersect in a line ℓ that intersects the supporting plane of e in x. Clearly, u and v must lie on ℓ since they are part of both quadrilaterals $abuv$ and $cduv$.

We consider two cases. In the first case, u and v lie on different halflines of ℓ with respect to x. Then vertices a, b, u, and v are in convex position, forming a convex quadrilateral with diagonals uv and ab. Note that it is not possible to connect points in convex position with straight-line segments to form a non-degenerate non-convex polygon. This contradicts the fact that all quadrilaterals in F must be non-convex. In the second case, u and v lie on the same halfline of ℓ with respect to x. But then vertices c, d, u, and v are in convex position since also c and d lie on the same halfline with respect to x. This again yields the desired contradiction. □

Proposition 3.5 *The Steiner quadruple system $S(3, 4, 10)$ does not admit a non-crossing drawing in 3D, where all quadrilaterals representing the hyperedges are convex or all quadrilaterals are non-convex.*

Proof: The Steiner quadruple system $S(3, 4, 10)$ has ten vertices and 30 hyperedges and is unique; see Table 2. Note that $S(3, 4, 10)$ satisfies the assumptions of Lemma 3.4 for $a = 1, b = 4, c = 2, d = 5, u = 7, v = 9, w = 6, x = 0, y = 3$, and $z = 8$, i.e., it contains the set of edges $F = \{1245, 1260, 4560, 1479, 2579, 1538, 2438\}$. The claim follows from Lemma 3.4. □

Theorem 3.6 *No Steiner quadruple system admits a non-crossing drawing using convex quadrilaterals in 3D. If the system contains at least 20 vertices, it does not admit a non-crossing drawing using any quadrilaterals in 3D.*

Proof: Day and Edelsbrunner [10, Lemma 2.3] used an approach similar to that of Carmesin (mentioned in footnote 3) to show that the number of triangles

spanned by n points in 3D is less than n^2 if no two triangles have a non-trivial intersection. (A trivial intersection is a common point or edge.) We need to redo their proof taking lower-order terms into account. If a Steiner quadruple system $S(3, 4, n)$ can be drawn using quadrilaterals in 3D, the intersection of these quadrilaterals with a small sphere around a vertex is a planar graph. Recall that any $S(3, 4, n)$ has n vertices and $m = \binom{n}{3}/4$ quadruples. Let v be any vertex. Then v is incident to $4m/n = (n-1)(n-2)/6$ quadrilaterals. Suppose that there is a representation consisting of only convex quadrilaterals. Break each convex quadrilateral incident to v into two triangles such that both triangles are incident to v. The intersection of these triangles with a small sphere around v yields a graph on $n-1$ vertices (that is, on all vertices but v) with $(n-1)(n-2)/3$ edges. For $n > 8$, this graph cannot be planar. This, together with Proposition 3.3, yields the first part of our claim.

The same approach proves the second part as well. Suppose that there is a representation without any restrictions. For a non-convex quadrilateral incident to v, it may or may not be possible to break it into two triangles such that both are incident to v. Here, we can only break the quadrilaterals (convex or non-convex) for which this splitting is possible. After this step, the polygons incident to v are either triangles or quadrilaterals. The intersection of these polygons with a small sphere around v yields a graph that has at most $n-1$ vertices and at least $(n-1)(n-2)/6$ edges. Such a graph cannot be planar for $n \geq 18$. Since the first Steiner quadruple system with $n \geq 18$ vertices has 20 vertices, the proof is complete. $\qquad\square$

3.2   Conclusion and Open Problems

We conclude the paper by pointing out some possible directions for further research.

Representing Graphs.   Our general construction in Section 2.1 implies that every n-vertex graph of maximum degree Δ can be represented in 3D by monotone polygonal curves with at most $\Delta - 2$ bends. Is there a natural class of graphs such that every graph G in that class can be represented by such chains with fewer than $\Delta(G) - 2$ bends?

Open Problem 3.7 *Does some non-trivial class of graphs admit an intersection representation in 3D using polygonal chains with less than $\Delta(G) - 2$ bends for any graph G in that class?*

Furthermore, it is interesting to consider representations of specific graph with highly regular polygons. In particular, we suggest the following extension of the result in Theorem 2.12.

Open Problem 3.8 *If $k \geq 5$ is odd, can C_k^2 be represented by touching unit squares?*

Steiner Triple Systems.   We have constructed non-crossing drawings of the two smallest such systems, $S(2, 3, 7)$ and $S(2, 3, 9)$, using triangles; see Proposition 3.1. What about larger Steiner triple systems?

Open Problem 3.9 *Does any Steiner triple system $S(2, 3, n)$ with $n \geq 13$ admit a non-crossing drawing using triangles in 3D?*

Steiner Quadruple Systems.   We have shown that no Steiner quadruple system admits a crossing-free drawing using convex quadrilaterals and that Steiner systems with exactly 8 or with at least 20 vertices do not admit crossing-free drawings using arbitrary quadrilaterals; see Theorem 3.6 and Proposition 3.3.

Open Problem 3.10 *Does any Steiner quadruple system with $n \in \{10, 14, 16\}$ vertices admit a non-crossing drawing using "mixed" quadrilaterals, that is, some convex, some not?*

Projective Planes.   Note that in Steiner quadruple systems many pairs of edges intersect in two vertices. In a projective plane, every pair of edges (called *lines*) intersects in exactly one vertex (*point*). So maybe this is easier? Recall that any projective plane fulfills the following axioms:

(P1) Given any two distinct points, there is exactly one line incident to both of them.

(P2) Given any two distinct lines, there is exactly one point incident to both of them.

(P3) There are four points such that no line is incident to more than two of them. (Non-degeneracy axiom)

Every projective plane has the same number of lines as it has points. The projective plane of order N, $PG(N)$, has $N^2 + N + 1$ lines and points and there are $N + 1$ points on each line, and $N + 1$ lines go through each point. Equivalently, we can see $PG(N)$ as the Steiner system $S(2, N + 1, N^2 + N + 1)$.

Note, however, that any contact representation of $PG(3)$ by convex quadrilaterals contains a contact representation of $S(2, 3, 9)$ by triangles: just drop one of the 13 quadruples of $PG(3)$ and remove its four vertices from all quadruples. This yields twelve triples with the property that any pair of vertices is contained in a unique triple (P1).

Observation 3.11 *Suppose that there is a realization of $PG(3)$ with convex quadrilaterals, then no two quadrilaterals are coplanar in such a realization.*

Proof: For the sake of contradiction, suppose that two quadrilaterals, q_1 and q_2, lie in the same plane Π in a realization R of $PG(3)$ with convex quadrilaterals. Every two quadrilaterals share exactly one vertex (P2), hence, we can write q_1 and q_2 as $q_1 = u_1 u_2 u_3 w$ and $q_2 = v_1 v_2 v_3 w$. Since every pair of vertices appears in exactly one quadrilateral (P1), each pair $u_i v_j$ with $i, j \in \{1, 2, 3\}$ is contained
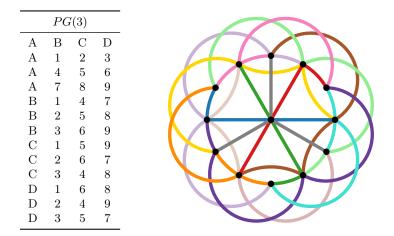
PG(3)			
A	B	C	D
A	1	2	3
A	4	5	6
A	7	8	9
B	1	4	7
B	2	5	8
B	3	6	9
C	1	5	9
C	2	6	7
C	3	4	8
D	1	6	8
D	2	4	9
D	3	5	7

Figure 18: The second smallest discrete projective plane $PG(3)$, which is a 4-regular 4-uniform hypergraph with 13 vertices and 13 hyperedges. The drawing was inspired by `https://puzzlewocky.com/games/the-math-of-spot-it/`.

in a different quadrilateral. Since the quadrilaterals in R are convex, each line segment $\overline{u_i v_j}$ is contained in the unique quadrilateral containing vertices u_i and v_j. Since u_i and v_j lie in Π, $\overline{u_i v_j}$ also lies in Π. As a result, Π contains a planar (straight-line) drawing of $K_{3,3}$ (with vertex set $\{u_1, u_2, u_3\} \cup \{v_1, v_2, v_3\}$), which yields the desired contradiction. $\qquad\square$

Or is it perhaps more natural to represent $PG(3)$ by touching tetrahedra? We used an integer linear program to compute the poset dimension of the vertex–hyperedge inclusion order of $PG(3)$, which turned out to be 5. Hence the method of Ossona de Mendez [22] yields a contact representation of $PG(3)$ by touching tetrahedra – but only in 4D.

Acknowledgments.

References

[1] M. J. Alam. *Contact Representations of Graphs in 2D and 3D*. PhD thesis, The University of Arizona, 2015.

[2] M. J. Alam, W. Evans, S. G. Kobourov, S. Pupyrev, J. Toeniskoetter, and T. Ueckerdt. Contact representations of graphs in 3D. In F. Dehne, J.-R. Sack, and U. Stege, editors, *Proc. Algorithms and Data Structures Symposium (WADS'15)*, volume 9214 of *LNCS*, pages 14–27, 2015. `doi: 10.1007/978-3-319-21840-3\_2`.

[3] M. J. Alam, M. Kaufmann, and S. G. Kobourov. On contact graphs with cubes and proportional boxes. In R. M. Freivalds, G. Engels, and B. Catania, editors, *Proc. 42nd Conf. Current Trends Theory & Pract. Comput. Sci. (SOFSEM'16)*, volume 9587 of *LNCS*, pages 107–120. Springer, 2016. `doi:10.1007/978-3-662-49192-8\_9`.

[4] U. Brandes, S. Cornelsen, B. Pampel, and A. Sallaberry. Path-based supports for hypergraphs. *J. Discrete Algorithms*, 14:248–261, 2012. `doi: 10.1016/j.jda.2011.12.009`.

[5] D. Bremner, W. Evans, F. Frati, L. Heyer, S. G. Kobourov, W. J. Lenhart, G. Liotta, D. Rappaport, and S. H. Whitesides. On representing graphs by touching cuboids. In W. Didimo and M. Patrignani, editors, *Proc. Int. Symp. Graph Drawing (GD'12)*, volume 7704 of *LNCS*, pages 187–198, 2012. `doi:10.1007/978-3-642-36763-2\_17`.

[6] K. Buchin, M. J. van Kreveld, H. Meijer, B. Speckmann, and K. Verbeek. On planar supports for hypergraphs. *J. Graph Algorithms Appl.*, 15(4):533–549, 2011. `doi:10.7155/jgaa.00237`.

[7] J. F. Canny. Some algebraic and geometric computations in PSPACE. In J. Simon, editor, *Proc. 20th Ann. ACM Symp. Theory Comput. (STOC'88)*, pages 460–467, 1988. `doi:10.1145/62212.62257`.

[8] J. Cardinal, S. Felsner, T. Miltzow, C. Tompkins, and B. Vogtenhuber. Intersection graphs of rays and grounded segments. *J. Graph Algorithms Appl.*, 22(2):273–295, 2018. `doi:10.7155/jgaa.00470`.

[9] J. Carmesin. Embedding simply connected 2-complexes in 3-space – I. A Kuratowski-type characterisation. ArXiv report, 2019. URL: `http://arxiv.org/abs/1709.04642`.

[10] T. K. Dey and H. Edelsbrunner. Counting triangle crossings and halving planes. *Discrete Comput. Geom.*, 12(3):281–289, 1994. `doi:10.1007/BF02574381`.

[11] K. Diks and P. Stańczyk. Perfect matching for biconnected cubic graphs in $O(n \log^2 n)$ time. In J. van Leeuwen, A. Muscholl, D. Peleg, J. Pokorný, and B. Rumpe, editors, *Proc. 36th Conf. Current Trends Theory &*

Pract. Comput. Sci. (SOFSEM'10), volume 5901 of *LNCS*, pages 321–333. Springer, 2010. `doi:10.1007/978-3-642-11266-9\_27`.

[12] J. Erickson and S. Kim. Arbitrarily large neighborly families of congruent symmetric convex 3-polytopes. In A. Bezdek, editor, *Discrete Geometry*, volume 253 of *Pure and Applied Mathematics*, pages 267–278. Marcel Dekker, New York, 2003. In Honor of W. Kuperberg's 60th Birthday.

[13] W. S. Evans, P. Rz1ażewski, N. Saeedi, C. Shin, and A. Wolff. Representing graphs and hypergraphs by touching polygons in 3d. In D. Archambault and C. D. Tóth, editors, *Graph Drawing and Network Visualization - 27th International Symposium, GD 2019, Prague, Czech Republic, September 17-20, 2019, Proceedings*, volume 11904 of *Lecture Notes in Computer Science*, pages 18–32. Springer, 2019. URL: `https://doi.org/10.1007/978-3-030-35802-0_2`, `doi:10.1007/978-3-030-35802-0\_2`.

[14] S. Felsner and M. C. Francis. Contact representations of planar graphs with cubes. In F. Hurtado and M. J. van Kreveld, editors, *Proc. 27th Ann. Symp. Comput. Geom. (SoCG'11)*, pages 315–320. ACM, 2011. `doi:10.1145/1998196.1998250`.

[15] H. Gropp. The drawing of configurations. In F. J. Brandenburg, editor, *Proc. Int. Symp. Graph Drawing (GD'95)*, volume 1027 of *LNCS*, pages 267–276. Springer, 1996. `doi:10.1007/BFb0021810`.

[16] P. Hliněný and J. Kratochvíl. Representing graphs by disks and balls (a survey of recognition-complexity results). *Discrete Mathematics*, 229(1–3):101–124, 2001. `doi:10.1016/S0012-365X(00)00204-1`.

[17] S. Ho0+1+1+1sten and W. D. Morris. The order dimension of the complete graph. *Discrete Math.*, 201(1):133–139, 1999. `doi:10.1016/S0012-365X(98)00315-X`.

[18] D. S. Johnson and H. O. Pollak. Hypergraph planarity and the complexity of drawing Venn diagrams. *J. Graph Theory*, 11(3):309–325, 1987. `doi:10.1002/jgt.3190110306`.

[19] P. Koebe. Kontaktprobleme der konformen Abbildung. *Berichte über die Verhandlungen der Sächsischen Akad. der Wissen. zu Leipzig. Math.-Phys. Klasse*, 88:141–164, 1936.

[20] J. Kratochvíl and J. Matoušek. Intersection graphs of segments. *J. Comb. Theory, Ser. B*, 62(2):289–315, 1994. `doi:10.1006/jctb.1994.1071`.

[21] J. Matoušek. Intersection graphs of segments and $\exists\mathbb{R}$. ArXiv report, 2014. URL: `http://arxiv.org/abs/1406.2636`.

[22] P. Ossona de Mendez. Realization of posets. *J. Graph Algorithms Appl.*, 6(1):149–153, 2002. `doi:10.7155/jgaa.00048`.

[23] J. Petersen. Die Theorie der regulären graphs. *Acta Math.*, 15:193–220, 1891. `doi:10.1007/BF02392606`.

[24] M. Schaefer. Complexity of some geometric and topological problems. In D. Eppstein and E. R. Gansner, editors, *Proc. 17th Int. Symp. Graph Drawing (GD'09)*, volume 5849 of *LNCS*, pages 334–344. Springer, 2010. `doi:10.1007/978-3-642-11805-0\_32`.

[25] W. Schnyder. Embedding planar graphs on the grid. In *Proc. 1st ACM-SIAM Symp. Discrete Algorithms (SODA'90)*, pages 138–148, 1990. URL: `https://dl.acm.org/citation.cfm?id=320176.320191`.

[26] C. Thomassen. Interval representations of planar graphs. *J. Combin. Theory Ser. B*, 40(1):9–20, 1986. `doi:10.1016/0095-8956(86)90061-4`.

[27] E. J. van Leeuwen and J. van Leeuwen. Convex polygon intersection graphs. In U. Brandes and S. Cornelsen, editors, *Proc. 18th Int. Symp. Graph Drawing (GD'10)*, volume 6502 of *LNCS*, pages 377–388. Springer, 2011. `doi:10.1007/978-3-642-18469-7\_35`.

[28] E. W. Weisstein. Steiner quadruple system. From MathWorld – A Wolfram Web Resource. Accessed 2019-08-20. URL: `http://mathworld.wolfram.com/SteinerQuadrupleSystem.html`.

[29] E. W. Weisstein. Steiner triple system. From MathWorld – A Wolfram Web Resource. Accessed 2019-08-20. URL: `http://mathworld.wolfram.com/SteinerTripleSystem.html`.

[30] J. Westbrook and R. E. Tarjan. Maintaining bridge-connected and bi-connected components on-line. *Algorithmica*, 7(1):433–464, 1992. `doi:10.1007/BF01758773`.

[31] A. A. Zykov. Hypergraphs. *Uspekhi Mat. Nauk*, 29(6):89–154, 1974. `doi:10.1070/RM1974v029n06ABEH001303`.